PLANT IDENTIFICATION USING COLOR CO-OCCURRENCE MATRICES

S. A. Shearer, ASSOC. MEMBER ASAE
R. G. Holmes, MEMBER ASAE

ABSTRACT

A method of identifying plants based on color texture characterization of canopy sections was developed. Color co-occurrence matrices were derived from image matrices, one for each color attribute: intensity, saturation, and hue. Eleven texture features were calculated from each of the co-occurrence matrices. The 33 total color texture features were used in a discriminant analysis model to identify plants. Overall classification accuracy of 91% was achieved when this method was used to identify seven common cultivars of nursery stock. A total of 350 observations were used in the investigation. This method exhibited a significant improvement over previous methods which used intensity data only.

INTRODUCTION

Machine vision is being used with much success in the automation of many manufacturing and quality control processes. Background and lighting are carefully controlled to produce high contrast images in a majority of these applications. Controlled settings coupled with consistent, well-known product geometries make object identification and location a relatively simple task. Due to the unstructured nature of typical agricultural settings and biological variation of plants within them, object identification in these applications is considerably more difficult. Thresholding, picture element (pixel) connectivity, template matching, and pattern recognition techniques used to identify objects within these scenes are useful in only a limited number of cases.

Previous work in the area of plant identification include a variety of approaches. Brazee and Fox (1973) used Walsh transforms to identify shape patterns of leaves. Kincaid and Schneider (1983) used a two-dimensional Fourier transform to quantify leaf shape. Guyer et al. (1984) segmented images with plants and soil background, and then using spatial features, were able to discern between plant species. More recently Franz et al. (1990) used a Fourier-Mellin correlation to identify both completely-visible and partially occluded leaf shapes. Franz et al. (1990) also used statistical measures from multiple wavebands to discriminate among leaf classes.

Article was submitted for publication in December 1989; reviewed and approved for publication by the Electrical and Electronic Systems Div. of ASAE in October 1990. Presented as ASAE Paper No. 87-1534.

The authors are **S. A. Shearer**, Assistant Professor, Agricultural Engineering Dept., University of Kentucky, Lexington; and **R. G. Holmes**, Professor, Agricultural Engineering Dept., Ohio Agricultural Research and Development Center, The Ohio State University, Columbus.

One obvious discriminating factor in agricultural settings is the difference in textural appearance of various plant canopies. This visual texture sensation results from the variation in reflected light from the plant canopy and it's surroundings. The purpose of this research was to investigate the feasibility of using visual texture sensation to identify objects within agricultural scenes.

Texture analysis is a well-developed technology and has been used for the analysis of all types of images. These range from microscopic images in the biomedical community to satellite images of the earth's surface. Most researchers have chosen to base their methods on the variation in relative intensity of reflected light. Surprisingly, researchers have altogether ignored the visual sensation of color. If the attributes describing color were included in texture analysis, a more accurate classification method might result.

Several approaches to texture analysis have been developed over the past 10 to 20 years. Researchers have attempted to compare methods, but at this point no studies have clearly identified the best approach. Haralick (1978) identified eight statistical approaches for the measurement and characterization of image texture which included: optical transforms, digital transforms, autocorrelation functions, autoregressive models, structural elements, textural edgeness, gray-level run lengths, and spatial gray-level co-occurrence probabilities.

The spatial gray-level dependence method (SGDM) was first reported by Julesz (1962) as a result of work with visual pattern discrimination. Haralick and Shanmugam (1973) used this principle for automatically classifying reservoir sandstones, using a procedure they termed "spatial gray-tone dependence matrices". Haralick, Shanmugam, and Dinstein (1973) also used the same approach to classify aerial photographs and satellite images. Haralick and Shanmugam (1974) further studied the possibility of combining spectral with spatial processing using the SGDM for classifying a set of Earth Resource Technology Satellite (ERTS) images.

Davis et al. (1978) extended the idea of spatial gray-level dependence by making the definition more general. Instead of looking at nearest neighbors, these authors identified several geometric constraints which defined neighborhoods. Zucker and Terzopolous (1980) proposed a statistical approach to determining the spatial relations which best capture the structure of textures. This method was intended for use with the SGDMs or as the authors termed them "co-occurrence matrices".

By combining color specification and the SGDM, several new texture descriptors are possible. This article proposes a new set of 33 texture features for describing

  0001-2351 / 90 / 3306-2037

color textures as further described by Shearer (1986). Color images of leaf canopies of seven cultivars of nursery stock were used to demonstrate classification power of this new approach.

Objectives

- To develop a method of automatically quantifying the color attributes of individual picture elements.
- To characterize visual plant canopy textures using color co-occurrence matrices.
- To verify the usefulness and accuracy of this approach for identifying plant canopy sections.

Color Determination Procedure

According to Nevatia (1982), humans are able to distinguish between colors using the three independent attributes: intensity, hue, and saturation. Intensity can be thought of as the attribute which is used to measure the brightness of achromatic light. Hue is often referred to as color. Red, yellow, and blue are examples of different hues. The third attribute, saturation, refers to the amount of white mixed with a pure hue.

In 1931 the International Commission on Illumination (CIE) proposed a standard method of color specification based on color matching principles using tristimulus values. Tristimulus values are the relative intensities of three different primary color spectra required to arouse the same color sensation as the light in question. If the spectrum of reflected light from a surface can be broken down into relative intensities of tristimulus colors, the color of the surface can be easily specified.

A method was needed to quickly multiply the spectrum curve by each of the tristimulus relative intensity curves and integrate the product. Eastman Kodak Company gelatin filters, approximately 0.1 mm in thickness, No. 25 (red), No. 58 (green), and No. 47B (blue) (Kodak, 1981) were used in combination with a vidicon tube camera to obtain tristimulus values directly. Unfortunately, the spectral response of the vidicon tube camera also acted as a filter. Figure 1 illustrates the tristimulus functions obtained from the product of the filter transmittance functions and the vidicon tube spectral response. Integration of these three curves was performed by a Panasonic model WV 1500 vidicon camera, the output signal voltage being proportional to the area under each of the three curves. The RS 170 camera signal was digitized and stored in memory on a Micro Works DS-65A video card. This card was capable of resolving an image with a resolution of 256 x 256 at 256 gray levels. The host micro computer was an Apple IIe manufactured by Apple Computer Incorporated.

After obtaining the tristimulus values, a transform was used to represent color. Ohta (1985) found that among seven sets of color features which are often used, only one expressed values relating to intensity, saturation, and hue. According to Ohta one problem associated with this set of features was the instability of hue for unsaturated colors, resulting when the sum of tristimulus values was small. To avoid this problem, a transform (refer to fig. 2) based on the CIE chromaticity diagram was used. With this method, intensity was defined as the average of the tristimulus values. In equation form, the intensity was represented as:

$$I = \frac{X + Y + Z}{3} \quad (1)$$

Chromaticity coordinates x and y were calculated for each pixel as:

$$x = \frac{X}{X + Y + Z} \quad (2)$$

$$y = \frac{Y}{X + Y + Z} \quad (3)$$

Assuming (x_R, y_R) represented the coordinates of a reference color and (x_P, y_P), the color of the pixel in question, hue was calculated as:

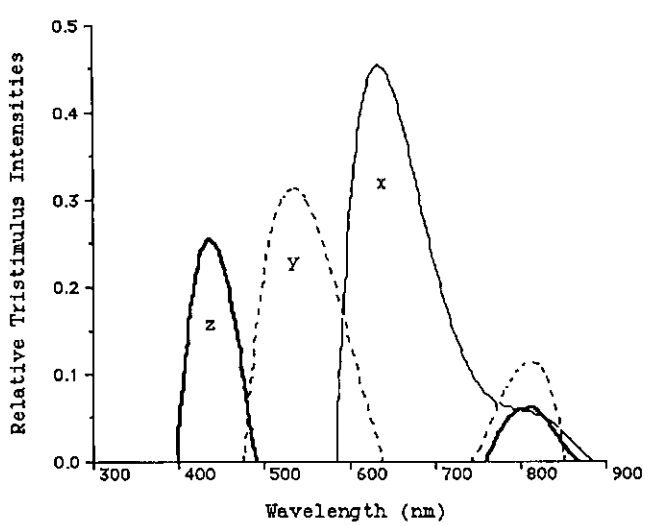

Figure 1–Tristimulus functions X, Y, and Z. These functions were obtained by multiplying the filter transmittances by the relative spectral response of the vidicon tube.

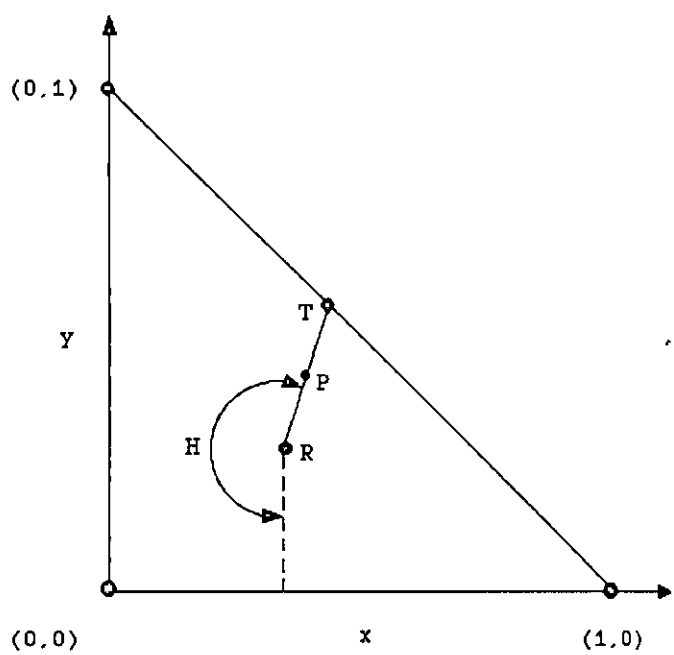

Figure 2–CIE color specification triangle. Triangle geometry with hue and saturation attributes are represented in the diagram.

$$H = \tan^{-1}\left(\frac{y_P - y_R}{x_P - x_R}\right) \quad (4)$$

A line was extended from point R through point P to the perimeter of the triangle and the intersection was labeled as T. Point T represented the maximum saturation (of the corresponding hue) detectable by this system. In equation form saturation was expressed as:

$$S = \frac{\overline{RP}}{\overline{RT}} \quad (5)$$

where $\overline{RP}$ and $\overline{RT}$ are the length of lines connecting points R and P, and point R and T, respectively.

For programming considerations it was desirable to represent intensity, saturation, and hue by integer values ranging from 0 to 63. Hue took on values from zero to 2π. This range was divided into 64 separate hue sectors. The selection of the zero sector was somewhat arbitrary. According to literature values from Kodak, the dominant wavelength for filters No. 25, No. 58, and No. 47B were 617.2, 538.2, and 452.7 nm, respectively, for illuminant A. Assuming hues were represented by dominant wavelengths, the hue of point (0,0) in figure 2 was equivalent to 452.7 nm, point (0,1) to 538.2 nm, and point (1,0) to 617.2 nm. This suggested that hue should be represented by increasing values in the clockwise direction from point (0,0) to (1,0). A vertical line downward through point R was selected as a starting point for specification of hue.

Color Co-occurrence Matrices and Texture Features

The SGDM measures the probability that a pixel at one particular gray-level will occur at distinct distance and orientation from any pixel given that pixel has a second particular gray-level. The SGDM matrices were represented by the function $P(i,j,d,\theta)$ where i represents the gray-level of location (x,y), and j represents the gray-level of the pixel at a distance d and an orientation of θ from location (x,y). In figure 3a, the reference pixel is denoted by an asterisk. The surrounding nearest neighbors were numbered 1 to 8 in a clockwise direction. These 8 neighbors represent all neighbors at a distance of 1. Neighbors 1 and 5 represented the neighboring pixels located at a distance of 1 in a horizontal direction from location (x,y). Extending this concept to additional orientations and summing the results over the entire image the SGDM matrices in figure 3c were obtained for the image matrix in figure 3b. These matrices were normalized by dividing each entry by the sum of entries in respective matrices.

Color co-occurrence matrices (CCM) were a direct extension of the SGDM matrices. Instead of having one SGDM matrix for each combination of d and θ, there were three. These matrices represented the co-occurrence of intensity, saturation, and hue attributes. The matrix for intensity was represented by the function $P_I(i,j,d,\theta)$ while $P_S(i,j,d,\theta)$ and $P_H(i,j,d,\theta)$ represented the saturation and hue matrices respectively. By using discretized values of intensity, saturation and hue, these matrices were treated as

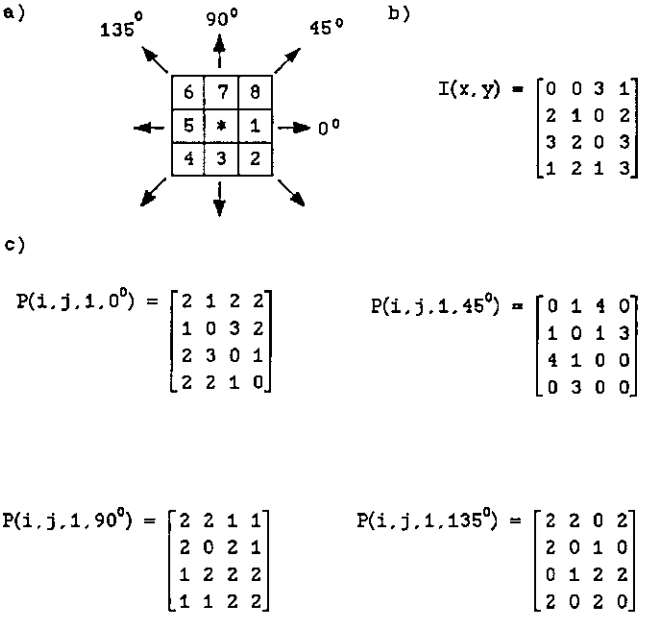

Figure 3–a) Nearest neighbor diagram. b) Simple gray-level image array. c) SGDM matrices at several orientations for the image array in a.

SGDM matrices. Feature extraction from the CCMs could then be repeated three times for each combination of d and θ. The 16 texture features as described by Haralick and Shanmugan (1973) would result in a total of 48 color texture features for each combination of d and θ.

For this study the co-occurrence matrices were derived by considering the eight nearest neighbors. Essentially, d was limited to 1 and all values of θ were included. Considering the eight nearest neighbors in the analysis created a unique situation where all of the co-occurrence matrices were symmetric with respect to the diagonal.

To reduce computation, it was desired to exclude redundant texture features. Haralick and Shanmugan (1973) stated that some of the texture features were highly correlated. This was not surprising, since the contrast and difference moment both measured the same property and were numerically equivalent. The difference moment and difference variance were found to be equivalent also. Additionally, the difference moment and the sum variance could be expressed as linear combinations of other features. These relationships were possible since the co-occurrence matrix was symmetric as defined above. For this reason the contrast, difference moment, sum variance, and difference variance texture features were omitted from the analysis. The maximum correlation coefficient was also omitted because of the extensive computational requirements.

The following texture features were calculated for each CCM:

Notation

Matrix normalization:

$$p(i,j) = \frac{P(i,j)}{\sum_{i=0}^{N_g-1}\sum_{i=0}^{N_g-1} P(i,j)} \quad (6)$$

Marginal probability matrix:

$$p_x(i) = \sum_{j=0}^{N_g-1} p(i,j) \quad (7)$$

Sum and difference matrices:

$$p_{x+y}(k) = \sum_{i=0}^{N_g-1} \sum_{\substack{j=0 \\ k=i+j}}^{N_g-1} p(i,j) \quad (8)$$

$$\text{for } k = 0,1,2,\ldots,2(N_g - 1)$$

$$p_{x-y}(k) = \sum_{i=0}^{N_g-1} \sum_{\substack{j=0 \\ k=|i-j|}}^{N_g-1} p(i,j) \quad (9)$$

$$\text{for } k = 0,1,2,\ldots,(N_g - 1)$$

where

$P(i,j)$ = the image attribute matrix, and

N_g = the total number of attribute levels (64).

Texture Features

Angular second moment:

$$f_1 = \sum_{i=0}^{N_g-1} \sum_{j=0}^{N_g-1} [\, p(i,j) \,]^2 \quad (10)$$

Mean:

$$f_2 = \sum_{i=0}^{N_g-1} i\, p_x(i) \quad (11)$$

Variance:

$$f_3 = \sum_{i=0}^{N_g-1} (i - f_2)^2 p_x(i) \quad (12)$$

Correlation:

$$f_4 = \frac{\sum_{i=0}^{N_g-1} \sum_{j=0}^{N_g-1} i\, j\, p(i,j) - f_2^{\,2}}{f_3} \quad (13)$$

Product moment:

$$f_5 = \sum_{i=0}^{N_g-1} \sum_{j=0}^{N_g-1} (i - f_2)(j - f_2)\, p(i,j) \quad (14)$$

Inverse difference moment:

$$f_6 = \sum_{i=0}^{N_g-1} \sum_{j=0}^{N_g-1} \frac{p(i,j)}{1 + (i - j)^2} \quad (15)$$

Entropy:

$$f_7 = \sum_{i=0}^{N_g-1} \sum_{j=0}^{N_g-1} p(i,j) \ln p(i,j) \quad (16)$$

Sum entropy:

$$f_8 = \sum_{k=0}^{2(N_g-1)} p_{x+y}(k) \ln p_{x+y}(k) \quad (17)$$

Difference entropy:

$$f_9 = \sum_{k=0}^{(N_g-1)} p_{x-y}(k) \ln p_{x-y}(k) \quad (18)$$

Information measures of correlation:

$$f_{10} = \frac{f_7 - HXY1}{HX} \quad (19)$$

$$f_{11} = \left[\, 1 - e^{-2(HXY2 - f_7)} \,\right]^{1/2} \quad (20)$$

where,

$$HX = -\sum_{i=0}^{N_g-1} p_x(i) \ln p_x(i) \quad (21)$$

$$HXY1 = -\sum_{i=0}^{N_g-1} \sum_{j=0}^{N_g-1} p(i,j) \ln [\, p_x(i)\, p_x(j) \,] \quad (22)$$

$$HXY2 = -\sum_{i=0}^{N_g-1} \sum_{j=0}^{N_g-1} p_x(i)\, p_x(j) \ln [\, p_x(i)\, p_x(j) \,] \quad (23)$$

Many of the texture features are indicative of texture traits perceived by humans such as contrast, coarseness, and others. A sense of what each texture feature represented is given next to aid in interpretation of the resulting values. The following discussion is based on Haralick and Shanmugan (1973) and the experience of the authors. Interpretations are confined to the intensity attribute of pixel color.

The angular second moment was a measure of the image homogeneity. Few intensity transitions are characteristic of homogeneous images. The result is a minimal number of entries of large magnitude in the co-occurrence matrix resulting in a high angular second moment. Conversely, numerous entries in the co-occurrence matrix produce a low second moment.

The mean intensity level was a measure of image brightness derived from the co-occurrence matrix. Alternatively, a similar measure could be obtained from a histogram of the intensity values for the image. Histograms are a very close approximation to the marginal probability matrix.

Variation of image intensity was identified by the variance texture feature. This is also very similar to the variance obtained from an intensity histogram. A higher numerical value indicates greater variability of the pixel intensities within the image. Conversely, a variance of zero would indicate that all pixels within the image have the same intensity.

Correlation was a measure of the intensity linear dependences in the image. The correlation of images with large areas of similar intensities will be higher than for noisier scenes. Since noise is uncorrelated, then these scenes would be represented by correlations of near zero.

The product moment was analogous to the covariance of the intensity co-occurrence matrix. Larger positive values of the product moment indicate that it is more likely for similar intensity levels to occur together. Negative values large in magnitude are indicative of images where neighboring pixels differ greatly in intensity values. The difference between the product moment and the correlation is that the correlation is a normalized measure. Both features tend to quantify the same characteristic.

Contrast of an image was measured by the inverse difference moment. The frequency of similar intensities occurring together were given a higher weighting than the frequency of extremely different intensities. For example, the frequency of two equal intensities occurring together is given a weight of 1 while the frequency of intensities differing by two is given a weight of 0.2.

The entropy feature was a measure of the amount of order in an image. For example, a black and white image where the left half is black and the right is white has a much lower entropy than if the image had a black and white checkerboard pattern. The first image would be said to have more order and, therefore, a lower entropy.

The sum and difference entropies were not as easily interpreted. The sum probability matrix comes from summing probabilities along the right diagonals of the co-occurrence matrix while the difference probability matrix comes from summing probabilities along the left diagonals. High entropies would be associated with images where entries in both the sum and difference matrices were evenly distributed. In both cases, low entropies would indicate high levels of order in both matrices.

The information measures of correlation did not exhibit any apparent physical interpretation with the exception that the first is a ratio of entropies.

Materials and Methods

The usefulness of the CCM approach for plant identification was demonstrated using seven cultivars of containerized nursery stock. The following seven cultivars were used:

1. Juniperus horizontalis 'Procumbens Nana' (Jap Garden Juniper)
2. Juniperus chinensis 'San Jose' (San Jose)
3. Juniperus horizontalis 'Wiltoni' (Blue Rug Juniper)
4. Chamaecy paris pisifera 'Boulevard' (Boulevard)
5. Taxus x media 'Hicksii' (Hicksii Taxus)
6. Rhododendron x 'Ramapo' (Ramapo)
7. Rhododendron x 'P.J.M.' (P.J.M.)

A total of 350 observations (50 observations from each cultivar) were used. No more than one observation was obtained from an individual plant. Thirty-five millimeter color photographs were made of each canopy section for logistical reasons and to insure a permanent record. Four BCA photoflood light bulbs in reflectors with diffuser covers were located symmetrically around individual plants to provide adequate and uniform lighting for the photography process. All pictures were taken inside white, poly covered greenhouses between the hours of 10 A.M. and 2 P.M. on two consecutive, sunny days. The reflector covers and poly greenhouse covering provided extremely diffuse lighting. As noted by Carroll (1970), some filtering of information occurred by the very nature of the photographic process. It was concluded that this was a relative shift that should not influence the overall results. All film was selected from the same lot and processed at the same time to reduce variation.

An image resolution of 64×64 was selected. The region of each photograph to be digitized was limited to 10.24 cm^2. This was the maximum continuous canopy available in all of the photographs taken. Therefore, each pixel represented an area of 0.0025 cm^2 in the photographs. Relating this resolution to the actual canopy, each pixel represented an area ranging from about 0.001 to about 0.021 cm^2 depending on vertical location in the canopy.

The tristimulus images were obtained by digitizing each canopy section three times using a different filtered illuminating light. Photographs were positioned between two plates of glass so that the denser part of the canopy covered the entire image window. No other particular orientation or positioning of the photographs was maintained. Figure 4 illustrates the illuminating and reflected light paths. A containerized plant is depicted in place of the photographs.

A gray card (Cat. No. 152 7795, Eastman Kodak Co.) was used as the reference color because of its reflectance properties. Between 400 and 700 nm the gray card reflected 18% of the incident radiation regardless of wavelength. For each color, the average values from all 4096 pixels were used as the tristimulus values of the reference. The reference X, Y, and Z values were 43.37, 29.27, and 24.16, respectively. CCMs were formed and normalized for each image. Texture features were calculated directly from these matrices.

To identify the texture features of each co-occurrence matrix the variable f was replaced by variables I, S, and H with appropriate subscripts. For example, texture features f_1 through f_{11} from the intensity co-occurrence matrix were represented as I_1 through I_{11}.

A distance measure computed with the SAS, DISCRIM option (SAS, 1982) was used to compute posterior probabilities for classification in each group. Observations were classified as belonging to the group for which the posterior probability was greatest. Using SAS procedures the data were divided into training and test sets. Starting with the first observation, every other observation was

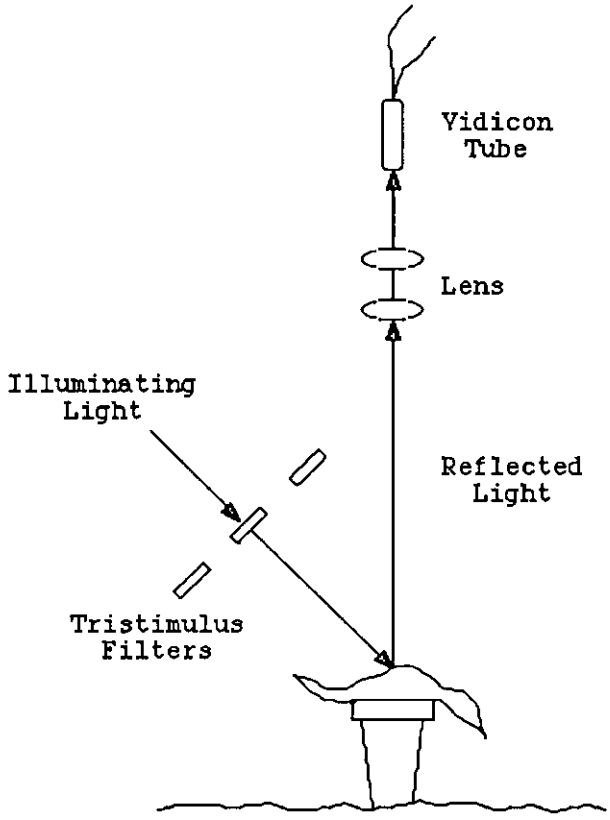

Figure 4–Modified tristimulus value, data collection scheme.

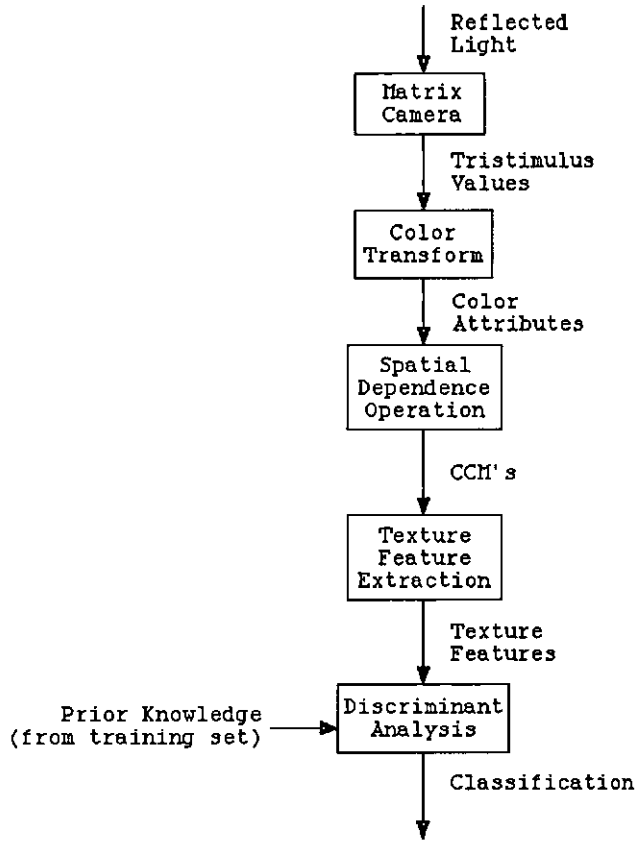

Figure 5–Color-texture plant identification flow chart.

selected for the training data set. This procedure resulted in a data set containing 175 observations, 25 from each cultivar. The alternate observations were grouped as the test data set. The training set was used to create the covariance matrices and the mean vectors used for the classification of the test data set. Figure 5 summarizes the overall approach to plant identification.

To aid in selecting texture features for various models, the SAS, STEPDISC procedure was used. STEPDISC was used on the intensity, saturation, and hue texture features separately, and then for all of the texture features together. The STEPWISE selection option added variables to the model according to two criteria; an F-test of the covariates, and a squared partial correlation to predict the variable under consideration from those already added to the model. In each run a significance level of 0.0001 was specified for the F-test to help guard against adding variables which did not contribute significantly to the discriminating ability of the model. Higher significance levels could have been used; however, it was the authors' intent to select models which minimized calculation.

Before presenting the results of the DISCRIM procedure, an example using two variables to discriminate between three cultivars is examined. The point of this example was to demonstrate the process by which DISCRIM classifies observations. The three classes chosen to be discriminated between were Jap Garden, Blue Rug, and Ramapo. From the training data sets of these cultivars, STEPDISC was used to select model variables. The first two variables selected by STEPDISC were used for the example. The DISCRIM option was run using variables I_{10} and H_2 and the training data sets of the Jap Garden, Blue Rug, and Ramapo cultivars. A test of homogeneity of within group covariance was performed and it was determined that within group covariance matrices should be used in the discriminant function instead of a pooled covariance matrix.

The generalized squared distance function used in the DISCRIM procedure was written as:

$$D_t^2 = (x - m_t)' S_t^{-1} (x - m_t) + \ln|S_t| \quad (24)$$

where

x = a vector containing the variable values of an observation,

m_t = a vector containing within class means of group t, and

S_t = the covariance matrix within group t.

Using this distance measure, the posterior probability of this observation belonging to each group was calculated with the SAS DISCRIM option as:

$$P_t(x) = \frac{e^{-0.5D_t^2(x)}}{\sum_n e^{-0.5D_u^2(x)}} \quad (25)$$

Figure 6 is a representation of how unknown observations from each class would be identified in the I_{10} - H_2 plane. The lines indicate equal probability of an

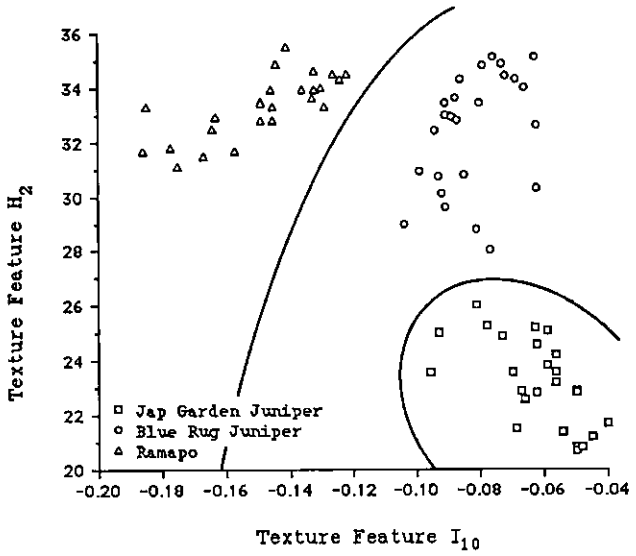

Figure 6–Discriminant analysis example results. The Jap Garden Juniper, Blue Rug, and Ramapo regions are separated with equi-probability lines. These lines represent a 0.5 probability of belonging to the class on either side.

observation belonging to the group on either side of the line. The positions of each of the 25 observations for the Jap Garden, Blue Rug, and Ramapo test data sets have been plotted. As a reminder, the equal-probability lines were obtained from the training data set. For this example, the classification of both the training and test data set was 100%. However, as the number of classes increased, the discrimination procedure became more complex and classification accuracies began to drop.

Results and Discussion

The repeatability of the data collection and processing procedure was evaluated by digitizing a San Jose canopy section 12 times. The intensity and saturation features were relatively stable. In contrast, the hue texture features exhibited a lot of variation. This variability can be attributed to the instability of the color transform at low saturations. When the chromaticity coordinates of the pixel in question were close to those of the reference color a slight variation in the tristimulus values introduced dramatic errors. Checking the image tristimulus values obtained from the DS-65 card it was not uncommon for each of them to vary by a value of 2 for the same pixel. The variation in the hue texture features were always less than the within class variation. It was concluded that the system repeatability was adequate and that good results could be obtained.

Development of discriminant analysis was based on normally distributed data. For this reason it was necessary to assess the normality of the data. Bar plots of each set of 50 within class texture features were created to check for possible bimodal or skewed distributions. Most of the texture features appeared normally distributed with the exception S_{10} and H_1 which were slightly skewed. A few transforms of the data such as natural log, square root, and raising the variable to higher powers were examined. While the transforms helped make the data from some cultivars appear more normally distributed, it actually skewed the data distributions of other cultivars. The Shapiro-Wilk statistic (W) as outlined in SAS (1985) was used to test the normality of the data. The W statistic ranges between 0 and 1.0 and is the ratio of the best estimator of the variance to the corrected sum of squares estimator. Higher values indicate acceptance of the null hypothesis; the data represents a random sample from a normally distributed population. The lowest W statistic for all within class texture features was 0.706. Ninety five percent (220 of 231) of the within class test statistics were above 0.9. In view of these results it was concluded the data was normally distributed.

All texture features have some discriminating power however small. In some cases, however, features actually decreased the discrimination power of the model. A second important factor is computation time. If a smaller set of texture features has an equal discrimination ability, then the overall computation can be reduced without loss of classification accuracy.

Six models were constructed using the results of STEPDISC. Models I through III were composed of only intensity, saturation, and hue features respectively. Model IV resulted from STEPDISC when all features were included. For comparison purposes, all features were included in model V. Model VI will be discussed later. Each model was then run using the DISCRIM option. In each case, the likelihood ratio test of homogeneity, for within group versus pooled covariance matrices, was found to be significant at the 0.10 level. Accordingly, the within group covariance matrices were used for calculation of the squared distance measures resulting in quadratic classifiers for each model. The same training and test data sets were used to evaluate each model. Both model specification and classification accuracy for training and test data sets are summarized in Table 1.

Hue features of model III performed comparably to the intensity features of model I for identification of the test data. It should also be noted that model III included only six features in contrast to the nine features of model I. Classification of the training data was about 10% greater for model I than III. Model II performed poorly when compared with models I and III, however it did show some promise. The true benefit of the CCM method versus the SGDM comes when both the intensity and hue features were combined. Model IV was derived by STEPDISC from all 33 features. Of the seven features selected, three were intensity and the remainder were hue. The test data

TABLE 1. Discriminant model classification accuracy

Model	Variables	% Classification accuracy	
		Training set	Test set
I	$I_1, I_2, I_3, I_5, I_6, I_7, I_9, I_{10}, I_{11}$	96.6%	81.7%
I	S_1, S_2, S_3, S_6, S_9	79.4%	64.0%
III	$H_1, H_2, H_3, H_5, H_6, H_7$	86.9%	81.1%
IV	$I_2, I_6, I_9, H_1, H_2, H_3, H_7, H_{11}$	96.6%	88.6%
V	$I_1, I_2, I_3, I_4, I_5, I_6, I_7, I_8, I_9, I_{10}, I_{11}, S_1, S_2, S_3, S_4, S_5, S_6, S_7, S_8, S_9, S_{10}, S_{11}, H_1, H_2, H_3, H_9, H_{10}, H_{11}$	100.0%	90.3%
VI	$I_2, I_6, I_9, H_2, H_3, H_7, H_{11}$	96.6%	90.9%

set was classified with an 88.6% accuracy representing a marked improvement over previous models. When all of the variables were included in model V, the training data set was classified with 100% accuracy, while the test data set classification increased to 90.3%.

In an effort to reduce calculations it was desirable to determine if reducing the number of variables included in the model would adversely affect the discrimination accuracy. As a guide, the results of the STEPDISC variable selection option was used. Since saturation features were not included, the computation required in the analysis of model VI was reduced by one third. Using model VI, a 90.9% classification accuracy of the test data set was achieved. This model represents the best choice of features when compared to the others because of the reduced processing and increased classification accuracy.

Model VI was compared to model I to determine if there was a significant improvement with the addition of hue to the analysis. Model I misclassified 21 observations which were identified correctly in model VI. Conversely, model VI misclassified 5 observations which model I classified correctly. To compare these two models the number of misclassified observations from each model were represented by a binomial distribution with 26 observations and a probability of 0.5. The null hypothesis of the test was that both models misclassified observations which the other model identified correctly, probability. The null hypothesis was rejected if the numbers of misclassified observations were either too large or too small. The significance level of this test was therefore stated as:

$$\alpha = P(N_I \geq 21 \mid H_0) + P(N_{VI} < 5 \mid H_0) \qquad (26)$$

where N_I and N_{VI} represent the number of misclassified observations correctly identified by the alternate model with respect to the subscripts. The null hypothesis was rejected at a significance level of 0.0025. This demonstrated the significant improvement in classification accuracy of model VI over model I.

Checking the original photographs of the misclassified observations revealed that several exhibited areas of less dense foliage within the canopies. This coupled with the chlorotic state of several plants contributed to the misclassification.

Conclusions

The following conclusions were drawn from this research:

1. By considering the hue variation of the canopies in the texture analysis, the classification accuracy is substantially increased when compared with intensity data only.
2. Careful selection of model features can drastically decrease processing requirements without loss of classification accuracy.

References

Brazee, R.D. and R.D. Fox. 1973. Transform representation of foliage. ASAE Paper No. 73-523. St. Joseph, MI: ASAE.

Carroll, J.S. 1970. *Amphoto Lab Handbook*. New York: American Photographic Book Publishing Co. Inc.

Davis, L., S.A. Johns and J.K. Aggarwal. 1978. Texture analysis using generalized co-occurrence matrices. *Proceedings on Pattern Recognition and Image Processing*, 313-318.

Franz, E., M.R. Gebhardt and K.B. Unklesbay. 1990. Shape description of completely-visible and partially-occluded leaves for identifying plants in digital images. ASAE Paper No. 90-7040. St. Joseph, MI: ASAE.

———. 1990. The use of local spectral properties of seedlings in digital images. ASAE Paper No. 90-7044. St. Joseph, MI: ASAE

Guyer, D.E., G.E. Miles and M.M. Schrieiber. 1984. Computer vision and image Processing for plant identification. ASAE Paper No. 84-1632. St. Joseph, MI: ASAE.

Haralick, R.M. and K. Shanmugam. 1973. Computer classification of reservoir sandstone. *IEEE Transactions on Geoscience Electronics* GE-11(14): 171-177.

———. 1974. Combined spectral and spatial processing of ERTS imagery data. *Journal of Remote Sensing of the Environment*. 3: 3-13.

Haralick, R.M., K. Shanmugam and I. Dinstein. 1973. Texture features for image classification. *IEEE Transactions on Systems, Man, and Cybernetics* SMC-3: 610-622.

Haralick, R.M. 1978. Statistical and structural approaches to texture. *Proceedings of the IEEE* 67(3): 786-804.

Julesz, B. 1962. Visual pattern discrimination. *IRE Transactions Information Theory* 8(2): 84-92.

Kincaid, D.T. and R.B. Schneider. 1983. Qualification of leaf shape with a microcomputer and Fourier transform. *Canadian Journal of Botany* 61(9): 2333-2342.

Kodak. 1981. *Kodak Filters for Scientific and Terminal*, 2nd ed. Eastman Kodak Co.

Nevatia, R. 1982. *Machine Perception*. Englewood Cliffs, NJ: Prentice Hall Inc.

Ohta, Y. 1985. *Knowledge-based Interpretation of Outdoor Natural Color Scenes*. Marshfield, MA: Pitman Publishing Inc.

SAS Institute Inc. 1982. SAS User's Guide: Statistics. Cary, NC: SAS Institute Inc.

Shearer, S.A. 1986. Plant identification using color co-occurrence matrices derived from digitized images. Unpublished Ph.D. diss. The Ohio State University, Columbus.

Zucker, S.W. and D. Terzopolous. 1990. Finding structure in co-occurrence matrices for texture analysis. *IEEE Proceedings on Computer Graphics and Image Processing* 12: 286-308.